Journal Pre-proofs

NW Iberian Peninsula coastal upwelling future weakening: competition between wind intensification and surface heating

Magda Catarina Sousa, Américo Ribeiro, Marisela Des, Moncho Gomez-Gesteira, Maite deCastro, João Miguel Dias

Please cite this article as: M.C. Sousa, A. Ribeiro, M. Des, M. Gomez-Gesteira, M. deCastro, J.M. Dias, NW Iberian Peninsula coastal upwelling future weakening: competition between wind intensification and surface heating, *Science of the Total Environment* (2019), doi: https://doi.org/10.1016/j.scitotenv.2019.134808

This is a PDF file of an article that has undergone enhancements after acceptance, such as the addition of a cover page and metadata, and formatting for readability, but it is not yet the definitive version of record. This version will undergo additional copyediting, typesetting and review before it is published in its final form, but we are providing this version to give early visibility of the article. Please note that, during the production process, errors may be discovered which could affect the content, and all legal disclaimers that apply to the journal pertain.

NW Iberian Peninsula coastal upwelling future weakening:

competition between wind intensification and surface heating

Magda Catarina Sousa[1*], Américo Ribeiro[1], Marisela Des[2], Moncho Gomez-Gesteira[2],

Maite deCastro[2], João Miguel Dias[1]

[1]CESAM, Departamento de Física, Universidade de Aveiro, 3810-193 Aveiro, Portugal

[2] Environmental Physics Laboratory (EphysLab), CIM-UVIGO, Universidade de Vigo, Edificio

Campus da Auga, 32004 Ourense, Spain

[*]*Corresponding Author:* M. C. Sousa. CESAM, Departamento de Física, Universidade de Aveiro, 3810-193 Aveiro,

Portugal. (mcsousa@ua.pt)

Abstract

Climate change will modify the oceanographic future properties of the NW Iberian Peninsula due to the projected variations in the meteorological forcing, that will intensify local winds and promote surface heating. The Delft3D-Flow model forced with atmospheric conditions provided within the framework of the CORDEX project under the RCP 8.5 greenhouse emission scenario was used to analyse changes in upwelling. Numerical experiments were conducted under high-extreme upwelling conditions for the historical (1976-2005) and future (2070-2099) period. This study also innovates through the exploitation of a numerical modelling approach that includes both shelf and estuarine processes along the coastal zone. Coastal upwelling will be less effective in the future despite the enhancement of upwelling favorable wind patterns previously predicted for this region. Upwelling weakening is due to the future sea

surface warming that will increase the stratification of the upper layers hindering the upward displacement of the underlying water, reducing the surface input of nutrients.

Keywords: *Global warming, coastal upwelling, stratification; estuary-near-shelf systems interaction, Delft3D, CORDEX, CMIP5*

1 Introduction

There is a worldwide concern about the possible impact of climate change on the circulation and hydrographic patterns of estuarine systems and their adjacent shelf. These changes can affect ecosystems in coastal upwelling areas whose response to surface warming is especially complex. Based on observational wind data, Bakun (1990) hypothesized that global warming could enhance land-sea temperature gradients that would consequently increase upwelling favorable winds. According to recent research, upwelling has increased over the last decades in most of the locations worldwide (Varela et al., 2015) and future projections indicate that upwelling will increase in intensity and duration at high latitudes over the next century (Wang et al., 2015), revealing more noticeable changes in the NW Iberian Peninsula (NWIP) (Sousa et al., 2017). Rykaczewski et al. (2015) and Sousa et al. (2017) showed that this upwelling strengthening is induced by the migration and intensification of the Azores High. On the other hand, the importance of coastal upwelling is twofold since apart from pumping nutrients to the surface, upwelling can also buffer global warming in coastal areas (Santos et al., 2012, 2011; Seabra et al., 2019; Varela et al., 2018). Stratification is also a key process to understand the link between climate change and biology since intensified stratification is negatively correlated with net primary

production (Behrenfeld et al., 2006; Manríquez et al., 2019). As a consequence of global warming, the upper ocean has warmed considerably over the last century and projections show that it will keep warming over this one (IPCC, 2013; Levitus et al., 2000). This fact will most likely increase ocean stratification, which can modify the behavior of the upper ocean in different ways. First, temperature anomalies in the upper ocean will penetrate to depth, but at slow rates and remaining confined near surface. Second, enhanced stratification will probably decrease, nutrient exchange through vertical mixing. Thus, increased thermal stratification can render less effective upwelling (García-Reyes et al., 2015; Gruber, 2011).

The NWIP coast is located in the northernmost limit of the Eastern North Atlantic Upwelling System, being characterized by a high primary production (Wooster et al., 1976). Changes in local primary production follow from changes in seawater temperature and salinity that depend on upwelling and freshwater discharge regimes resulting from estuary-near-shelf systems interaction. These drivers are likely to be modified in the future due to climate change. The NWIP coast includes three estuarine systems with different morphologies: high-relief estuaries or drowned river valleys (*Rias Baixas*: Rias de Vigo, Pontevedra, Arousa and Muros); estuaries connected to the major rivers (Minho, Lima and Douro) and a lagoon-estuarine system (*Ria de* Aveiro) (Figure 1). These estuarine systems are located in the northernmost part of one of the major coastal upwelling systems, being this process the main responsible of the steep-temperature gradient observed between coastal and ocean locations (Santos et al., 2011). On the other hand, the propagation of buoyant plumes, mostly from Douro and Minho rivers, dominates surface layers (Mendes et al., 2016). In summary, both river discharges and winds affect strongly the dynamics of these coupled estuary-near-shelf systems. This fact is especially patent for the *Rias Baixas* (Alvarez et al., 2006;

3

deCastro et al., 2006; Des et al., 2019; Otero et al., 2013; Sousa et al., 2014a, 2014b), where the upwelled water promotes the intense aquaculture (Blanton et al., 1987; Figueiras et al., 2002; Prego et al., 2001). Estuarine circulation and productivity have also been studied for the Minho, Lima, Douro and Ria de Aveiro estuaries (Alvarez et al., 2013; Costa-Dias et al., 2010; Dias and Picado, 2011; Mendes et al., 2013; Queiroga, 2003; Sousa et al., 2011; Vale and Dias, 2011; Vieira and Bordalo, 2000).

As far as we know, there is limited research on future changes in coastal upwelling systems, which can only be identified through the exploitation of fine horizontal and vertical resolution nearshore data. However, that resolution is far from the one provided by the ocean models used in IPCC (2013), which have typical horizontal and vertical resolutions around 1° and on the order of tens of meters, respectively, which are too coarse to reproduce coastal processes. Previous studies based on basin-scale or global circulation models have analyzed the impact of climate change along the coast of Iberian Peninsula (Miranda et al., 2013; Pires et al., 2013, 2015), but were only focused on the shelf. These studies analyzed upwelling changes based on IPCC A2 emission scenario and indicated an increase in coastal upwelling, supporting the idea initially proposed by Bakun (1990). However, a number of limitations contribute to keep the problem of future upwelling changes largely open. As example, most of previous studies based on model applications for NWIP present severe restrictions if used to evaluate climate change impacts, since they were typically implemented under unrealistic conditions neglecting the estuary-near-shelf systems interaction (Pires et al., 2013, 2015) or in the best considering the interaction with a single estuary (Lopes et al., 2017; Mendes et al., 2013). Moreover, simulations were performed using only a single ocean model, and some of the control results were found to be unsatisfactory, with an overestimation of the present climate upwelling mainly attributable to inaccuracies in

4

the wind data associated to the control simulation. In fact, Soares et al. (2012) highlighted the need to use higher resolution atmospheric simulations to represent topographic and coastal processes accurately. Thus, adopting the regional climate models projections from the 5th Assessment Report (AR5) of the IPCC scenarios (IPCC, 2013) to force the oceanographic models seems to be a valuable alternative to achieve the required level of accuracy to describe near-shore processes.

The present work aims at analysing the response of the NWIP coastal waters to future changes projected under the RCP 8.5 greenhouse gas emission scenario. These changes, which are characterized by air and water warming and the increase in upwelling favourable winds will be used to force the Delft3D-Flow model covering both the shelf and the estuaries in order to assess whether or not future wind and stratification patterns will modify the impact of upwelling in the area.

Figure 1: Here

2 Methodology

2.1 Numerical model

Delft3D-Flow modeling system was used to evaluate the impact of climate change on coastal upwelling along the NWIP coast. Delft3D-Flow is a three-dimensional, finite differences hydrodynamic and transport model. The Navier Stokes shallow water equations are solved with hydrostatic, Boussinesq and f-plane approximations (Deltares, 2014). The model was previously implemented and validated for the area under study by Sousa et al. (2018), which demonstrated its skill and high accuracy in reproducing the local coastal dynamics.

The configuration developed consists in a set of five domains connected by internal domain decomposition boundaries with the capability of two-way communication of water level, currents and hydrographic properties (Figure 1). These different types of domain discretization recognize the importance of using adaptive resolution meshes. The horizontal resolution of each domain allows reproducing the hydrodynamic of the areas covered, which in many cases have a complex geometry, without a high computational cost. The outer grid includes the continental shelf with a resolution of about ~1500 m. Douro and Ria de Aveiro were covered by two separated domains with a grid resolution varying from 45 to 80 m. Minho and Lima estuaries are combined into a single domain with a ~60 m grid resolution. The Rias Baixas are represented by a single domain with a horizontal resolution of ~250 m and thirteen vertical sigma layers with refined surface layers were used for all domains. The numerical bathymetry of each estuary was obtained from the interpolation of topohydrographic data from several different sources. The bathymetry of ocean, adjacent shelf and the Rias Baixas was generated from data from the General Bathymetry Chart of the Oceans. Minho, Lima and Douro bathymetries were generated from data available at the Portuguese Navy Hydrographic Institute, and the Ria de Aveiro bathymetry was generated from data provided by the Aveiro Harbor Administration and Polis Litoral Ria de Aveiro.

Thirteen main tidal harmonic constants (M_2, S_2, N_2, K_2, K_1, O_1, P_1, Q_1, M_sF, MM, M_4, MS_4, MN_4) obtained from the model TPXO 7.2 TOPEX/Poseidon Altimetry with a spatial resolution of ~25 km (MacMillan et al., 2004) were prescribed as astronomical forcing at the oceanic open boundary. Transport conditions (salinity and water temperature) were also imposed at this boundary based on monthly global climate models (GCM) from Coupled Model Intercomparison Project Phase 5 (CMIP5). The surface boundary condition was modelled considering daily wind, air temperature,

relative humidity and cloudiness provided by CMIP5 atmospheric models. Freshwater discharge for the major tributaries in the Rias Baixas and the Ria de Aveiro and for Minho, Lima and Douro rivers were imposed as fluvial open boundary conditions in each estuary, and were retrieved from the Hype Web portal (http://hypeweb.smhi.se/). A detailed description of the data used as boundary conditions will be described in the next section.

A k-ε model was used for 3D turbulence. A constant manning value of 0.024 was assumed for bottom roughness, except for Ria de Aveiro domain where a spatial variable friction coefficient (Lopes and Dias, 2015) was used due to the shallowness of the lagoon. The vertical eddy viscosity and diffusivity applied was 0.0001 m^2 s^{-1}, whereas a spatially variable horizontal viscosity and diffusivity proportional to the depth was applied, with a value of 5 m^2 s^{-1} in the inner domains (lowest depth) increasing linearly to 15 m^2 s^{-1} in the deepest ocean.

2.2 Climate forcing data

Near surface zonal and meridional wind components, near-surface air temperature, cloud cover, relative humidity and surface air pressure data were obtained from daily Regional Climate Models (RCM) simulations performed within the framework of the CORDEX initiative, with a resolution of 12.5 km. The EURO-CORDEX branch (http://www.euro-cordex.net/) downscales global climate simulations from the CMIP5 long experiments up to the year 2100 (Taylor et al., 2012). For the purposes of this study, the required variables were retrieved from nine RCMs simulations (Table 1) corresponding to the RCP8.5 scenario and assessed for the historical period. These regional simulations were obtained by means of three RCMs forced by six different GCMs (Table 1). A statistical analysis of each atmospheric variable was carried out to

determine the most accurate climate model in reproducing past climatic conditions. This analysis compares the dataset obtained from ERA-Interim with the ones provided by RCMs predictions over the historical period (1979-2005). The evaluation is based on the probability density functions (PDFs) and a simple quantitative measure of how efficiently each climate model can capture the observed PDFs for each variable. Thus, a skill score was used to evaluate the PDFs at daily scale:

$$S_{Score} = \sum_{i=1}^{n} minimum\ (Z_m^i, Z_o^i) \quad (1)$$

where Z_m^i and Z_o^i are the predicted and observed probability values of each bin and n is the number of bins. S_{Score} calculates the cumulative minimum value of observed and modeled distributions for each bin, quantifying the overlap between two PDFs (Perkins et al., 2007; Watterson, 2008). Values of S_{Score} equal to one indicate that model simulates the observed conditions perfectly. Hereafter, the mean S_{Score} for each climate simulation was computed, allowing to choose the best model to be used as surface boundary condition in modeling simulations.

The unavailability of ocean data (salinity and water temperature) from RCMs justifies the use of GCM predictions as oceanic boundary conditions. The criterion for selecting the most suitable GCM consists in choosing the same model that forces the best RCM.

Table 1: Here

2.3 Numerical scenarios

The first step in the definition of the numerical scenarios consists in determining the most suitable wind to force the hydrodynamic model. The protocol, which was used both for the historical (1976-2005) and the future (2070-2099) periods, can be summarized as follows: i) Eight control points located 20 km west from the mouth of

each estuary, in order to avoid winds measured on land, were selected; ii) Ekman transport and upwelling index (UI) were calculated at those points following the methodology adopted by Gomez-Gesteira et al. (2006).; iii) UI percentiles ranging from 75% to 99% (P7599 from now on) were determined at daily scale for the most upwelling favorable months (July and August) (Alvarez et al., 2008); (iv) the mean daily zonal and meridional wind corresponding to that interval of percentiles were calculated for each grid point in order to generate a space-varying domain. This procedure was only applied for the most accurate model, which was selected as described in last section. In summary, this approach identifies the wind conditions that characterize future and historical high-extreme upwelling events (percentile 75-99). In order to discard outliers, values higher than 99% were not considered. Space-varying winds were imposed in the simulation event.

A wind statistical analysis was performed considering a Weibull distribution to find the typical wind speed for both climate periods. The Weibull scale parameters are 6.4 and 6.6 m s^{-1} for historical and future climate periods, respectively. Thus, a constant wind speed of 6 m s^{-1} and clockwise direction (changing 45° per hour) was imposed for the spin-up both for historical and future period. As for wind direction, any rotation can be considered (clockwise, counter-clockwise or even random) as far as wind does not blow for a long time (several consecutive hours) from the same direction. The aim of this unusual wind regime is twofold, on the one hand, it allows heat diffusion between the ocean and the atmosphere and, on the other hand, it does not impose a dominant surface-driven circulation pattern (e.g. upwelling and downwelling) due to its continuous change in direction. In summary, at the end of spin-up the initial pattern is characterized by the thermal stratification imposed by the atmosphere in absence of

prevailing winds. This allows identifying the supplementary effect of upwelling on that initial configuration.

The transport properties at the oceanic open boundary were determined through the computation of a climatological mean for the favorable months for the historical (1976-2005) and future (2070-2099) periods. The same procedure was carried out for the remaining atmospheric variables (except the wind).

Regarding the river discharges, for the historical period a climatological mean (1981-2010) was also computed (Hundecha et al., 2016). For future simulation, it was found that the most pessimistic prediction anticipated a reduction of 25% in river discharges in this region (https://hypeweb.smhi.se/explore-water/climate-impacts/europe-climate-impacts/), hence, this reduction was considered for the historical climatological values previously obtained. This river discharge reduction is in accordance with the reduction of annual precipitation observed by Collins et al. (2013) and Cardoso Pereira et al. (2019) under the RCP8.5 scenario.

To determine the duration of the simulation, a statistical analysis was performed based on the identification of the high-extreme summer (P7599) upwelling events, revealing that they last from 4 to 6 days. Thus, a 5- day upwelling event preceded by a spin-up period of 3 weeks was simulated under the conditions described above.

3   Results and Discussion

3.1 Climate model evaluation

The skill of the climate model to reproduce real data was quantified by means of the S_{Score} for each atmospheric variable (Figure 2a). The S_{Score} is higher than 0.5 for all models and atmospheric variables. As mentioned above, the score measures the overlap

between two PDFs in such way that when it is equal to one the predicted and observed distributions are identical. In addition, the mean S_{Score} for each climate simulation was computed (Figure 2b) to determine the most accurate climate model in reproducing past climatic conditions. The mean S_{Score} for most RCMs (except models #1 and #4) remains above 0.7, indicating that these models can reproduce accurately the data distribution found in observations. The highest mean S_{Score} (0.81) was found for model #7 (MOHC-HadGE2-Es-RCA4), which showed the best fit between predictions and observations. According to these results, surface and open boundary conditions from the RCM MOHC-HadGEM2-Es-RCA4 and GCM MOHC-HadGEM2-Es, respectively, were used as initial and boundary conditions for the model.

Figure 2: Here

3.2 Climate change impact on coastal upwelling

Predicted sea surface temperature (SST) time-averaged (5 days) was computed for the study region for both climate periods (past and future) (Figure 3).

Figure 3: Here

For the historical climate period (Figure 3a), the mean SST shows the typical coastal upwelling pattern, with a strip of cold water along the NWIP coast, more intense between Douro estuary and north of Cape Finisterre. This was compared with Alvarez et al. (2012) results derived from satellite observations from 1998 to 2007, revealing a very similar pattern, which demonstrates the ability of the model developed. Concerning the future period (Figure 3b), the SST pattern is similar to the one observed for the historical period (Figure 3a), although the SST will be significantly higher (> 2 ºC) in the future. This increase in SST is consistent with the results reported for the same area but using GCMs from CMIP3 (Pires et al., 2015), and in other important upwelling

areas such as California (Xiu et al., 2018) and Humboldt Upwelling Systems (Oyarzún and Brierley, 2019) where the most significant warming was observed at the surface of the water column. The increase of the ocean temperatures will lead to changes that can affect ocean ecosystems and biogeochemical processes that are strongly dependent on temperature (Gruber, 2011).

The upwelling imprint between the end and the beginning of the upwelling event (ΔSST= SSTend - SSTbeginning) is quantified in Figure 4 for both periods. The area adjacent to the NWIP shows a clear SST drop between the end and the beginning of the upwelling event, as it would be expected due to the cooling of surface water induced by upwelling (Figure 4). This drop is even more marked nearshore and agrees with the difference between coast and near the adjacent ocean zone observed by Santos et al. (2011) at the NWIP and Varela et al. (2018) for most of the world coasts and especially in upwelling systems. Overall, patterns are similar for both climate periods in most of the domain, with the exception of the region between 41º 30' N and 42º 15' N, where nearshore values ranging from 2 to 3 °C were observed for the historical period, and from 1 to 2 °C for the future (Figures 4a and 4b). Both patterns are a clear proxy of the imprint of high-extreme upwelling events on coastal SST. Thus, the more negative the ΔSST, the more efficient the upwelling mechanism.

Figure 4: Here

Figure 5 shows the difference between the SST drop for the future and for the historical period, which is positive for most of the coastal domain north of 41º 30' N and zero for the rest. Positive (red) values indicate that the SST drop is lower for the historical period. This figure shows that despite the strengthening of UI north of 41.5°, which was described by Sousa et al. (2017) using future wind projections, the upward pumping of subsurface water is less effective. These results suggest that other factors apart from

wind, like the stratification of the water column prior to the upwelling event should be also considered.

Figure 5: Here

Figure 6 shows UI and water column stratification, described in terms of the Brunt-Väisälä frequency (N), for the domain between Minho and Ria de Vigo (pink box in Figure 1). As expected, higher UI values were observed for the future (red line in Figure 6a). However, water column stratification is higher for the surface mixed layer in the future (Figure 6c) compared to the historical period (Figure 6b). Near coast, the highest N values occur between 5 and 15 m depth for the historical period (Figure 6b) and between 5 and 25 m for the future (Figure 6c). Thermocline will be deeper and more intense in the future, which will increase the stratification in the whole section. This result is consistent with previous studies derived from numerical models forced with GCMs from CMIP3 (Pires et al., 2015) and CMIP5 (Oerder et al., 2015; Oyarzún and Brierley, 2019) projects. Oyarzún and Brierley (2019) verified that as ocean stratification increases upwelling of coastal seawaters sourced from 100 m to at 300 m depth becomes less connected to the wind stress. Thereby, the observed increase in stratification counteracts the intensification of upwelling favourable winds, which results in a decrease of intensity and frequency of upwelling events in the NWIP coast, as observed by Di Lorenzo et al. (2005) for the California Current System. Ocean stratification decreases the upper ocean mixing and transport, which in turns reduces the ability of the oceans to supply the oxygen from the surface into the thermocline (Gruber, 2011). Furthermore, the stratification will limit the subsurface-water upwelled to the sea surface, leading to warmer SST and limiting the nutrient influx. Ocean warming can then have a negative impact on the productivity of the NWIP coast, as described in (Gutierrez et al., 2011), Roemmich and McGowan (1995) for the

California Current, where the deepening of the thermocline resulted in the decline of zooplankton production. Additionally, Brochier et al. (2013), using an ocean numerical model, also showed that global warming could reduce the fish capacity in the Humboldt Current system.

Figure 6: Here

4 Conclusions

A realistic configuration of Delft3D-Flow was used to analyse present and future coastal upwelling along the NWIP coast. Firstly, the best atmospheric model to force Delft3D was chosen among the models provided by the CORDEX project. The accuracy of the models to reproduce past climate was assessed in terms of the Perkins analysis, pointing the RCM MOHC-HadGEM2-Es-RCA4 and the GCM MOHC-HadGEM2-Es, as the best candidates to force Delft3D. Numerical experiments were conducted under high-extreme upwelling conditions for two climate periods: a historical period (1976- 2005) and a far future period (2070-2099) under the RCP 8.5 greenhouse emission scenario. Despite wind induced upwelling forcing is projected to intensify during this century, the upwelling imprint, defined in terms of the water-cooling during high-extreme events, will be less intense in the future. This decrease in the effectiveness of upwelling is due to the future increase in the thermal stratification of the water column, which will limit the amount of deeper water that will reach the sea surface in the future. This fact can deeply affect the primary production and, consequently, influence the marine fish stocks.

14

Acknowledgements

References

Alvarez, I., deCastro, M., Gomez-Gesteira, M., Prego, R., 2006. Hydrographic behavior of the Galician Rias Baixas (NW Spain) under the spring intrusion of the Mino

River. Journal of Marine Systems 60, 144–152. https://doi.org/DOI
10.1016/j.jmarsys.2005.12.005

Alvarez, I., Dias, J.M., DeCastro, M., Vaz, N., Sousa, M.C., Gómez-Gesteira, M., 2013.
Influence of upwelling events on the estuaries of the north-western coast of the
Iberian Peninsula. Marine and Freshwater Research 64.
https://doi.org/10.1071/MF12298

Alvarez, I., Gomez-Gesteira, M., Decastro, M., Dias, J.M., 2008. Spatiotemporal
evolution of upwelling regime along the western coast of the Iberian Peninsula.
Journal of Geophysical Research-Oceans 113. https://doi.org/Artn C07020Doi
10.1029/2008jc004744

Alvarez, I., Lorenzo, M.N., deCastro, M., 2012. Analysis of chlorophyll a concentration
along the Galician coast: seasonal variability and trends. Ices Journal of Marine
Science 69, 728–738. https://doi.org/DOI 10.1093/icesjms/fss045

Bakun, A., 1990. Global Climate Change and Intensification of Coastal Ocean
Upwelling. Science 247, 198–201. https://doi.org/DOI
10.1126/science.247.4939.198

Behrenfeld, M.J., O'Malley, R.T., Siegel, D.A., McClain, C.R., Sarmiento, J.L.,
Feldman, G.C., Milligan, A.J., Falkowski, P.G., Letelier, R.M., Boss, E.S., 2006.
Climate-driven trends in contemporary ocean productivity. Nature 444, 752–755.
https://doi.org/10.1038/nature05317

Blanton, J.O., Tenore, K.R., Castillejo, F., Atkinson, L.P., Schwing, F.B., Lavin, A.,
1987. The Relationship of Upwelling to Mussel Production in the Rias on the
Western Coast of Spain. Journal of Marine Research 45, 497–511.

Brochier, T., Echevin, V., Tam, J., Chaigneau, A., Goubanova, K., Bertrand, A., 2013.
Climate change scenarios experiments predict a future reduction in small pelagic

fish recruitment in the Humboldt Current system. Global Change Biology 19, 1841–1853. https://doi.org/10.1111/gcb.12184

Cardoso Pereira, S., Marta-Almeida, M., Carvalho, A.C., Rocha, A., 2019. Extreme Precipitation Events under Climate Change in the Iberian Peninsula. International Journal of Climatology joc.6269. https://doi.org/10.1002/joc.6269

Collins, M., R. Knutti, J. Arblaster, J.-L. Dufresne, T. Fichefet, P. Friedlingstein, X. Gao, W.J. Gutowski, T. Johns, G. Krinner, M. Shongwe, C. Tebaldi, A.J. Weaver and M. Wehner, 2013: Long-term Climate Change: Projections, Com - mitments and Irreversibility. In: Climate Change 2013: The Physical Science Basis. Contribution of Working Group I to the Fifth Assessment Report of the Intergovernmental Panel on Climate Change [Stocker, T.F., D. Qin, G.-K. Plattner, M. Tignor, S.K. Allen, J. Boschung, A. Nauels, Y. Xia, V. Bex and P.M. Midgley (eds.)]. Cambridge University Press, Cambridge, United Kingdom and New York, NY, USA.

Costa-Dias, S., Freitas, V., Sousa, R., Antunes, C., 2010. Factors influencing epibenthic assemblages in the Minho Estuary (NW Iberian Peninsula). Marine Pollution Bulletin 61, 240–246. https://doi.org/DOI 10.1016/j.marpolbul.2010.02.020

deCastro, M., Alvarez, I., Varela, M., Prego, R., Gomez-Gesteira, M., 2006. Mino River dams discharge on neighbor Galician Rias Baixas (NW Iberian Peninsula): Hydrological, chemical and biological changes in water column. Estuarine Coastal and Shelf Science 70, 52–62. https://doi.org/DOI 10.1016/j.ecss.2006.05.035

Deltares, 2014. Delft3D-FLOW. Simulation of multi-dimensional hydrodynamic flows and transport phenomena, including sediments. User Manual. Hydro-Morphodynamics. Version: 3.15.34158, Delft3D Modeling Suite.

Des, M., deCastro, M., Sousa, M.C., Dias, J.M., Gómez-Gesteira, M., 2019.

Hydrodynamics of river plume intrusion into an adjacent estuary: The Minho River and Ria de Vigo. Journal of Marine Systems 189, 87–97. https://doi.org/10.1016/j.jmarsys.2018.10.003

Di Lorenzo, E., Miller, A.J., Schneider, N., McWilliams, J.C., 2005. The Warming of the California Current System: Dynamics and Ecosystem Implications. Journal of Physical Oceanography 35, 336–362. https://doi.org/10.1175/JPO-2690.1

Dias, J.M., Picado, A., 2011. Impact of morphologic anthropogenic and natural changes in estuarine tidal dynamics. Journal of Coastal Research 1490–1494.

Figueiras, F.G., Labarta, U., Fernández Reiriz, M.J., 2002. Coastal upwelling, primary production and mussel growth in the Rías Baixas of Galicia, in: Hydrobiologia. pp. 121–131. https://doi.org/10.1023/A:1021309222459

García-Reyes, M., Sydeman, W.J., Schoeman, D.S., Rykaczewski, R.R., Black, B.A., Smit, A.J., Bograd, S.J., 2015. Under Pressure: Climate Change, Upwelling, and Eastern Boundary Upwelling Ecosystems. Frontiers in Marine Science 2. https://doi.org/10.3389/fmars.2015.00109

Gomez-Gesteira, M., Moreira, C., Alvarez, I., Decastro, M., 2006. Ekman transport along the Galician coast (northwest Spain) calculated from forecasted winds. Journal of Geophysical Research-Oceans 111. https://doi.org/Artn C10005Doi 10.1029/2005jc003331

Gruber, N., 2011. Warming up, turning sour, losing breath: Ocean biogeochemistry under global change. Philosophical Transactions of the Royal Society A: Mathematical, Physical and Engineering Sciences. https://doi.org/10.1098/rsta.2011.0003

Gutierrez, D., Bouloubassi, I., Sifeddine, A., Purca, S., Goubanova, K., Graco, M., Field, D., Mejanelle, L., Velazco, F., Lorre, A., Salvatteci, R., Quispe, D., Vargas,

G., Dewitte, B., Ortlieb, L., 2011. Coastal cooling and increased productivity in the main upwelling zone off Peru since the mid-twentieth century. Geophysical Research Letters 38. https://doi.org/Artn L07603Doi 10.1029/2010gl046324

Hundecha, Y., Arheimer, B., Donnelly, C., Pechlivanidis, I., 2016. A regional parameter estimation scheme for a pan-European multi-basin model. Journal of Hydrology: Regional Studies 6, 90–111. https://doi.org/10.1016/j.ejrh.2016.04.002

IPCC, 2013. Climate Change 2013: The Physical Science Basis.Contribution of Working Group I to the Fifth Assessment Report of the Intergovernmental Panel on Climate Change , Stocker, T.F., D. Qin, G.-K. Plattner, M. Tignor, S.K. Allen, J. Boschung, A. Nauels, Y. Xia, V. Bex and P.M. Midgley (eds.). Cambridge University Press, Cambridge, United Kingdom and New York, NY, USA.

Levitus, S., Antonov, J.I., Boyer, T.P., Stephens, C., 2000. Warming of the world ocean. Science 287, 2225–2229. https://doi.org/10.1126/science.287.5461.2225

Lopes, C.L., Alves, F.L., Dias, J.M., 2017. Flood risk assessment in a coastal lagoon under present and future scenarios: Ria de Aveiro case study. Natural Hazards 89, 1307–1325. https://doi.org/10.1007/s11069-017-3025-x

Lopes, C.L., Dias, J.M., 2015. Assessment of flood hazard during extreme sea levels in a tidally dominated lagoon. Natural Hazards 77, 1345–1364. https://doi.org/10.1007/s11069-015-1659-0

MacMillan, D.S., Beckley, B.D., Fang, P., 2004. Monitoring the TOPEX and Jason-1 microwave radiometers with GPS and VLBI wet zenith path delays. Marine Geodesy 27, 703–716. https://doi.org/10.1080/01490410490904780

Mendes, Renato, Sousa, M.C., deCastro, M., Gómez-Gesteira, M., Dias, J.M., 2016. New insights into the Western Iberian Buoyant Plume: Interaction between the Douro and Minho River plumes under winter conditions. Progress in

Oceanography 141, 30–43. https://doi.org/10.1016/j.pocean.2015.11.006

Mendes, R., Vaz, N., Dias, J.M., 2013. Potential impacts of the mean sea level rise on
the hydrodynamics of the Douro river estuary. Journal of Coastal Research.
https://doi.org/10.2112/si65-330.1

Miranda, P.M.A., Alves, J.M.R., Serra, N., 2013. Climate change and upwelling:
response of Iberian upwelling to atmospheric forcing in a regional climate
scenario. Climate Dynamics 40, 2813–2824. https://doi.org/DOI 10.1007/s00382-
012-1442-9

Oerder, V., Colas, F., Echevin, V., Codron, F., Tam, J., Belmadani, A., 2015. Peru-
Chile upwelling dynamics under climate change. Journal of Geophysical Research:
Oceans 120, 1152–1172. https://doi.org/10.1002/2014JC010299

Otero, P., Ruiz-Villarreal, M., García-García, L., González-Nuevo, G., Cabanas, J.M.,
2013. Coastal dynamics off Northwest Iberia during a stormy winter period. Ocean
Dynamics 63, 115–129. https://doi.org/DOI 10.1007/s10236-012-0585-x

Oyarzún, D., Brierley, C.M., 2019. The future of coastal upwelling in the Humboldt
current from model projections. Climate Dynamics 52, 599–615.
https://doi.org/10.1007/s00382-018-4158-7

Perkins, S.E., Pitman, A.J., Holbrook, N.J., McAneney, J., 2007. Evaluation of the AR4
climate models' simulated daily maximum temperature, minimum temperature,
and precipitation over Australia using probability density functions. Journal of
Climate 20, 4356–4376. https://doi.org/10.1175/JCLI4253.1

Pires, A.C., Nolasco, R., Rocha, A., Dubert, J., 2013. Assessing future climate change
in the Iberian Upwelling System. Journal of Coastal Research 1909–1914.
https://doi.org/10.2112/SI65-323.1

Pires, A.C., Nolasco, R., Rocha, A., Ramos, C., Dubert, J., 2015. Climate change in the

Iberian Upwelling System: a numerical study using GCM downscaling. Climate Dynamics 1–14.

Prego, R., Dale, A.W., deCastro, M., Gomez-Gesteira, M., Taboada, J.J., Montero, P., Villareal, M.R., Perez-Villar, V., 2001. Hydrography of the Pontevedra Ria: Intra-annual spatial and temporal variability in a Galician coastal system (NW Spain). Journal of Geophysical Research-Oceans 106, 19845–19857.

Queiroga, H., 2003. Wind forcing of crab megalopae recruitment to an estuary (ria de aveiro) in the northern portuguese upwelling system. Invertebrate Reproduction and Development 43, 47–54. https://doi.org/10.1080/07924259.2003.9652521

Roemmich, D., McGowan, J., 1995. Climatic warming and the decline of zooplankton in the California current. Science 267, 1324–1326. https://doi.org/10.1126/science.267.5202.1324

Rykaczewski, R.R., Dunne, J.P., Sydeman, W.J., Garcia-Reyes, M., Black, B.A., Bograd, S.J., 2015. Poleward displacement of coastal upwelling-favorable winds in the ocean's eastern boundary currents through the 21st century. Geophysical Research Letters 42, 6424–6431. https://doi.org/10.1002/2015GL064694

Santos, F., DeCastro, M., Gómez-Gesteira, M., Allvarez, I., 2012. Differences in coastal and oceanic SST warming rates along the Canary upwelling ecosystem from 1982 to 2010. Continental Shelf Research 47, 1–6. https://doi.org/10.1016/j.csr.2012.07.023

Santos, F., Gomez Gesteira, M., deCastro, M., 2011. Coastal and oceanic SST variability along the western Iberian Peninsula. Continental Shelf Research 31, 2012–2017. https://doi.org/10.1016/j.csr.2011.10.005

Seabra, R., Varela, R., Santos, A.M., Gómez-Gesteira, M., Meneghesso, C., Wethey, D.S., Lima, F.P., 2019. Reduced Nearshore Warming Associated With Eastern

Boundary Upwelling Systems. Frontiers in Marine Science 6.
https://doi.org/10.3389/fmars.2019.00104

Soares, P.M.M., Cardoso, R.M., Miranda, P.M.A., Viterbo, P., Belo-Pereira, M., 2012.
Assessment of the ENSEMBLES regional climate models in the representation of
precipitation variability and extremes over Portugal. Journal of Geophysical
Research-Atmospheres 117. https://doi.org/Artn D07114Doi
10.1029/2011jd016768

Sousa, M.C., Alvarez, I., Vaz, N., Dias, J.M., 2011. Physical forcing of the hydrography
of the Ria de Vigo mouth. Journal of Coastal Research SI64, 1589–1593.

Sousa, M.C., deCastro, M., Alvarez, I., Gomez-Gesteira, M., Dias, J.M., 2017. Why
coastal upwelling is expected to increase along the western Iberian Peninsula over
the next century? Science of the Total Environment 592.
https://doi.org/10.1016/j.scitotenv.2017.03.046

Sousa, M.C., Ribeiro, A.S., Des, M., Mendes, R., Alvarez, I., Gomez-Gesteira, M.,
Dias, J.M., 2018. Integrated High-resolution Numerical Model for the NW Iberian
Peninsula Coast and Main Estuarine Systems. Journal of Coastal Research 66–70.
https://doi.org/10.2112/SI85-001.1

Sousa, M.C., Vaz, N., Alvarez, I., Gomez-Gesteira, M., Dias, J.M., 2014a. Modeling the
Minho River plume intrusion into the Rias Baixas (NW Iberian Peninsula).
Continental Shelf Research 85, 30–41.

Sousa, M.C., Vaz, N., Alvarez, I., Gomez-Gesteira, M., Dias, J.M., 2014b. Influence of
the Minho River plume on the Rias Baixas (NW of the Iberian Peninsula). Journal
of Marine Systems 139, 248–260.

Taylor, K.E., Stouffer, R.J., Meehl, G.A., 2012. An Overview of Cmip5 and the
Experiment Design. Bulletin of the American Meteorological Society 93, 485–498.

https://doi.org/Doi 10.1175/Bams-D-11-00094.1

Vale, L.M., Dias, J.M., 2011. The effect of tidal regime and river flow on the hydrodynamics and salinity structure of the Lima Estuary: Use of a numerical model to assist on estuary classification. Journal of Coastal Research 1604–1608.

Varela, R., Alvarez, I., Santos, F., deCastro, M., Gomez-Gesteira, M., 2015. Has upwelling strengthened along worldwide coasts over 1982-2010? Scientific Reports 5. https://doi.org/Artn 10016Doi 10.1038/Srep10016

Varela, R., Lima, F.P., Seabra, R., Meneghesso, C., Gómez-Gesteira, M., 2018. Coastal warming and wind-driven upwelling: A global analysis. Science of the Total Environment 639, 1501–1511. https://doi.org/10.1016/j.scitotenv.2018.05.273

Vieira, M.E.C., Bordalo, A.A., 2000. The Douro estuary (Portugal): a mesotidal salt wedge. Oceanologica Acta 23, 585–594. https://doi.org/Doi 10.1016/S0399-1784(00)01107-5

Wang, D.W., Gouhier, T.C., Menge, B.A., Ganguly, A.R., 2015. Intensification and spatial homogenization of coastal upwelling under climate change. Nature 518. https://doi.org/Doi 10.1038/Nature14235

Watterson, I.G., 2008. Calculation of probability density functions for temperature and precipitation change under global warming. Journal of Geophysical Research Atmospheres 113. https://doi.org/10.1029/2007JD009254

Wooster, W.S., Bakun, A., Mclain, D.R., 1976. Seasonal Upwelling Cycle Along Eastern Boundary of North-Atlantic. Journal of Marine Research 34, 131–141.

Xiu, P., Chai, F., Curchitser, E.N., Castruccio, F.S., 2018. Future changes in coastal upwelling ecosystems with global warming: The case of the California Current System. Scientific Reports 8. https://doi.org/10.1038/s41598-018-21247-7

Figure Legends:

Figure 1: Location and bathymetry of the study area. Black boxes correspond to the domain decomposition design. The shaded pink area indicates the location of the cross sections used to compute the upwelling index and the Brunt-Väisälä frequency.

Figure 2: S_{Score} for air temperature (Tair), air cloudiness (cloud), zonal (u) and meridional (v) components of wind, relative humidity (hum) and surface pressure (sp) for each model (a). Mean S_{Score} of all variables for each model (b).

Figure 3: Mean sea surface temperature under high-extreme upwelling conditions (P7599) for the historical (a) and future (b) periods.

Figure 4: SST drop between the end and the beginning of the upwelling event ($\Delta SST= SST^{end} - SST^{beginning}$) under high-extreme upwelling conditions (P7599) for the historical (a) and future (b) periods. This increment shows the upwelling imprint under both conditions.

Figure 5: Difference between historical and future upwelling imprint under high-extreme upwelling conditions (P7599) (calculated subtracting the historical from the future imprint $\Delta SST^{future} - \Delta SST^{historical}$).

Figure 6: Upwelling index corresponding to historical (black) and future conditions (a). Brunt-Väisälä frequency (N) prior to the upwelling event for the historical (b) and future (c) period. Values were calculated for the domain marked with a shaded area in Figure 1.
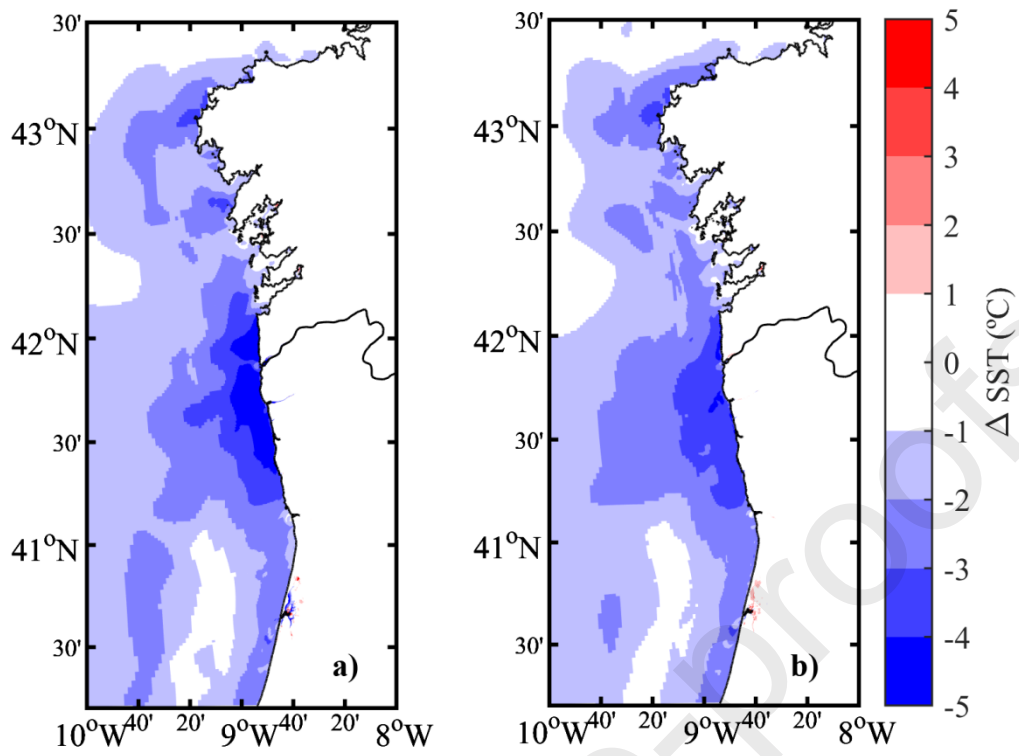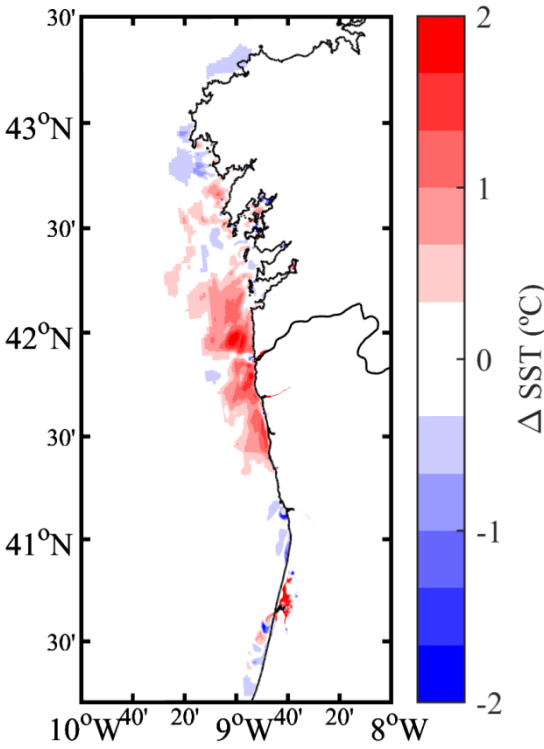
Table Legends:

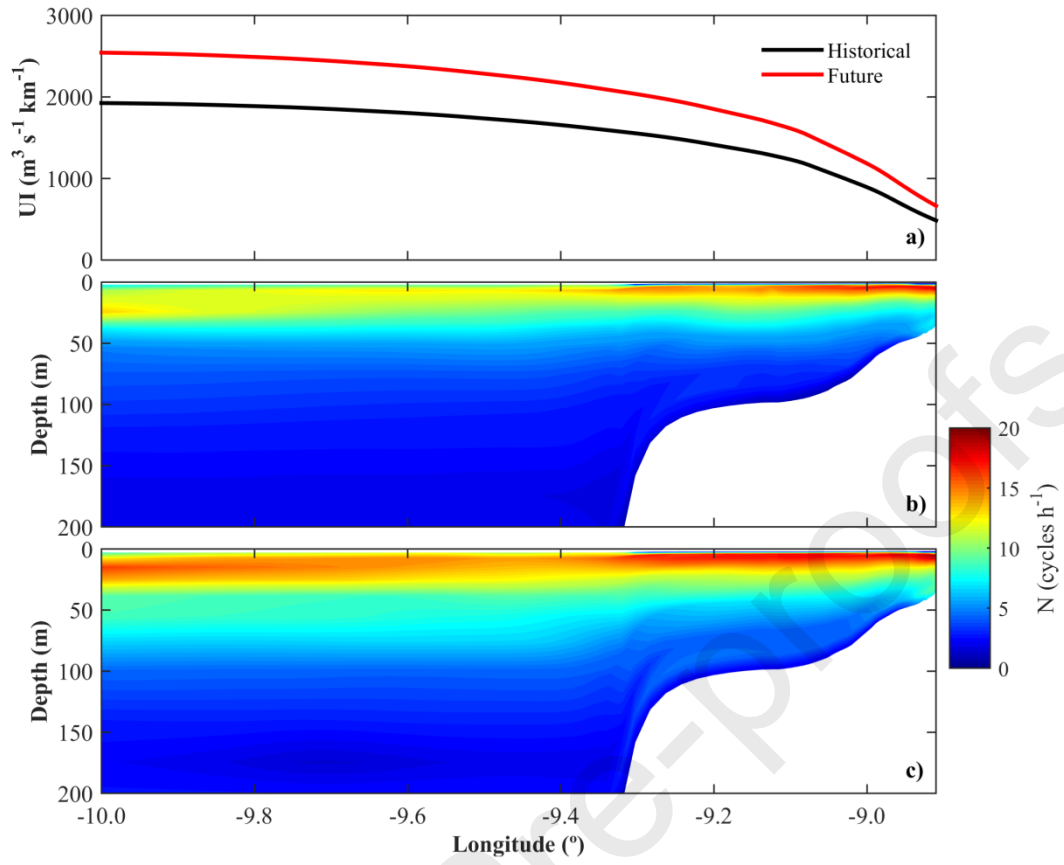**Table 1:** EURO Cordex simulations. Numbers in brackets correspond to model number shown in Figure 2.
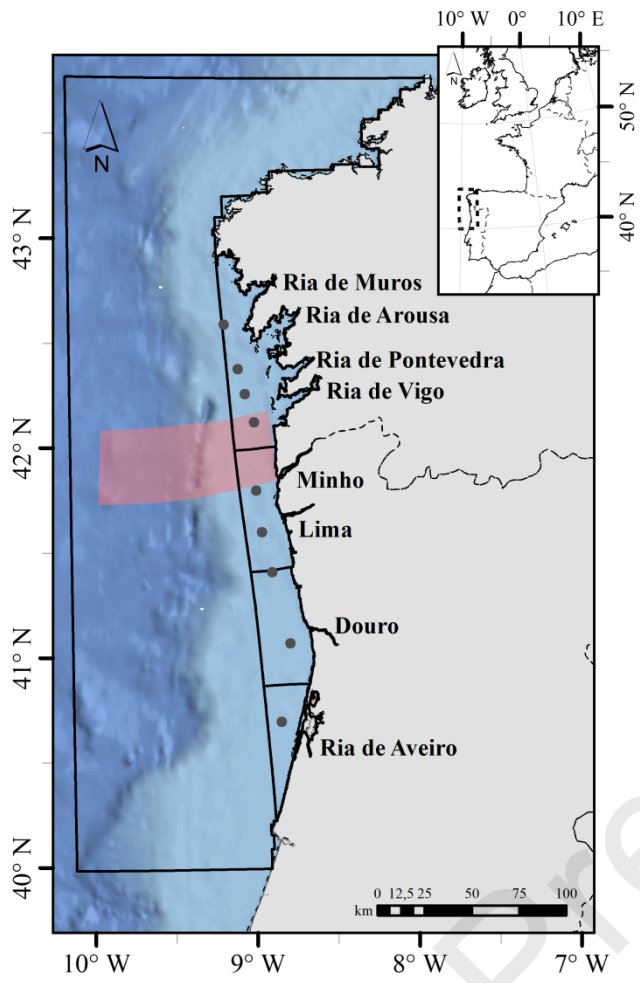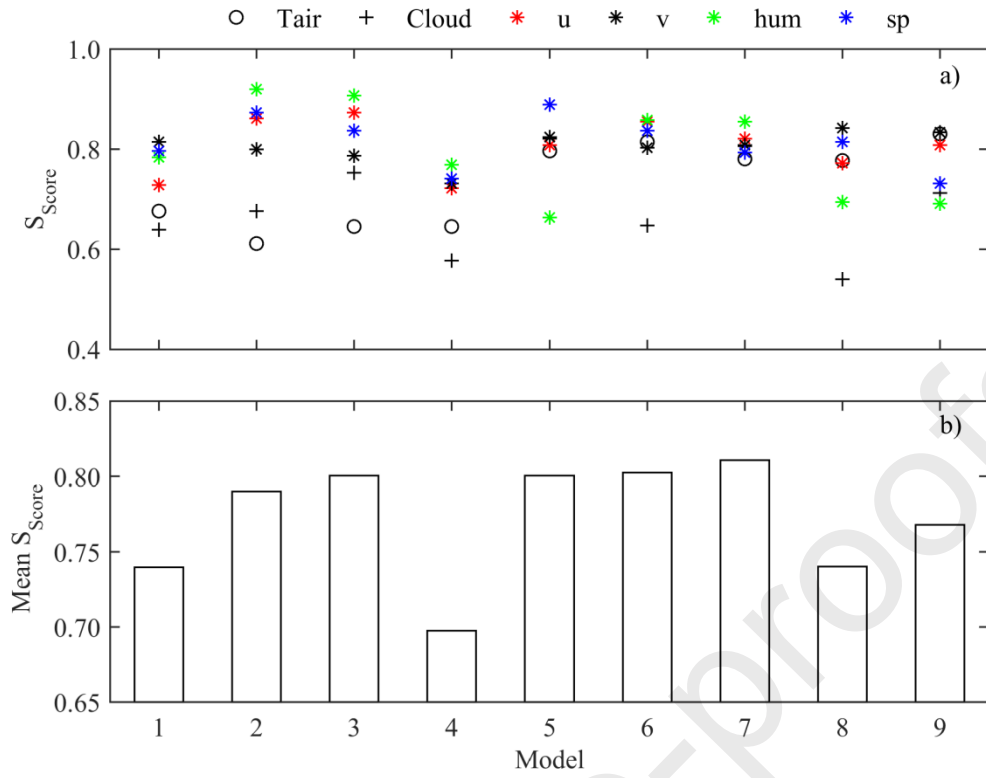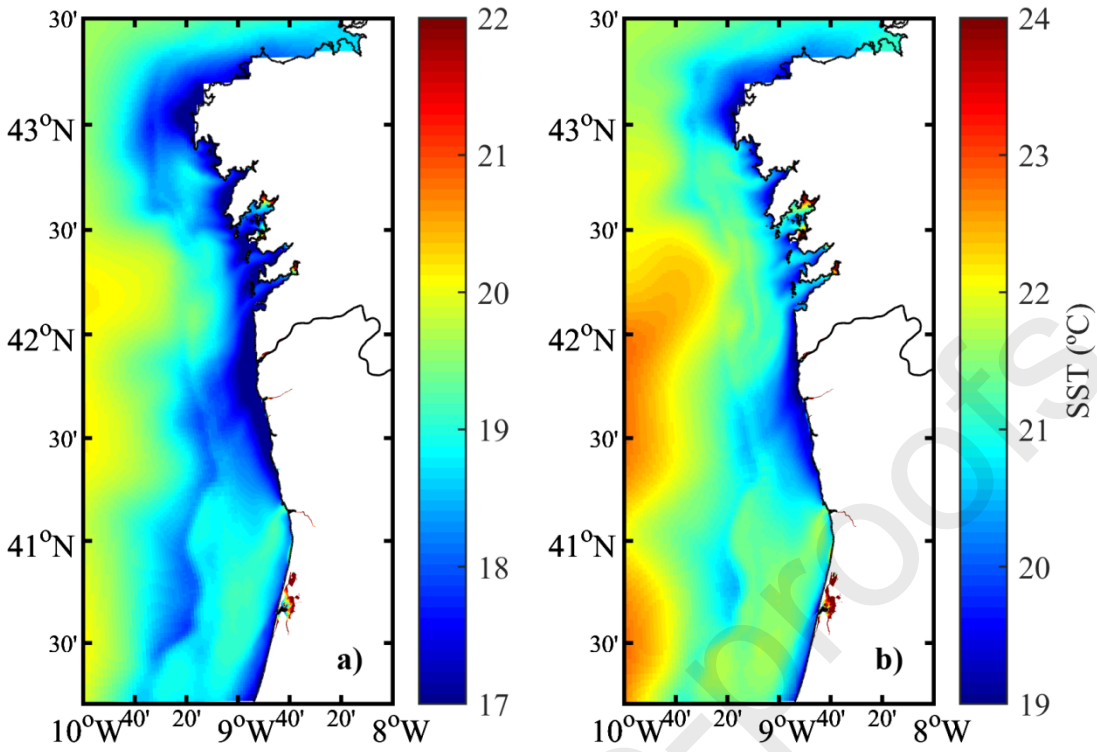
Table 2

GCM \ RCM	RACMO22E	HIRHAM5	RCA4
CNRM-CM5			X[1]
EC-EARTH	X[2]		X[3]
IPSL-CM5A-MR			X[4]
MOHOC-HadGEM2-ES	X[6]	X[5]	X[7]
MPI-ESM-LR			X[8]
NorESM-M		X[9]	

31

Highlights

- Most accurate climate model selection to reproduce past climatic conditions

- Realistic configuration including interaction between shelf and estuarine processes

- Coastal upwelling less effective in the future

- Upwelling weakening due to the future sea surface warming

Highlights